Grain sorting effects on the formation of sand waves

T. Van Oyen & P. Blondeaux
DICAT University of Genoa, Genoa, Italy

ABSTRACT: A model is proposed to investigate the initial formation of tidal sand waves considering a heterogeneous bed composition. The model is based on the study of the stability of the flat bottom configuration, i.e. small amplitude bottom perturbations are added to a flat bed and a linear analysis of their time development is carried out. Hiding/exposure effects on the fractional sediment transport rate are considered and a sediment continuity equation using the active layer concept is used. For moderate tidal currents, a graded sediment mixture tends to stabilize the flat bed configuration with respect to the case of uniform sediment and the sand waves that appear are longer. Moreover, a coarsening of the sediment at the crests and a fining at the troughs is found. Describing the heterogeneous mixture with more or less grain size classes appears to have no effect on the results.

1 INTRODUCTION

Recently, theoretical models have been developed to analyse the effects of a graded sediment on the formation of large scale tidal bedforms, stimulated by field surveys which show that quite often the sea bottom is made up of sediment mixtures characterized by a wide probability density distribution. Moreover, field observations reveal spatial variations of the mean grain size along tidal bedforms, indicating sorting processes (Swift et al. 1978, Antia 1996, Roos et al. 2007b). For instance, along the Middelkerke Bank (Belgian coast) the distribution of the mean grain size shows the accumulation of the coarser sediment on the crests and of the finer sediment in the troughs (Houthuys et al. 1994, Lanckneus et al. 1994, Vincent et al. 1998). Also data from the more seaward located Kwinte Bank (Gao et al. 1994) indicate a similar grain size pattern and variations in the mean grain size are also found for more onshore located coastal banks (Van Lancker 1999).

As described by Roos et al. (2007b), an overview of the grain size patterns over tidal sand waves in the southern part of the North Sea shows that at some locations (site 1, near Zandvoort; site 2, offshore of Egmond and Zee; site 4, near Hoek van Holland) the mean grain size at the crests is coarser than that at the troughs but at other locations (site 3, on Brown Bank; site 5, on the Thorton Bank) the sediment is coarser at the troughs.

Previous works have already pointed out the significance of a heterogeneous bed composition on the formation of coastal bedforms. For instance, the theoretical and experimental work of Foti & Blondeaux (1995a,b) shows that, if the sediment is graded, sea ripples appear for higher values of the Shields parameter than those characterizing a well sorted sediment and the ripple wavelength tends to be longer. Other works consider the effects of a graded sediment on shoreface-connected ridges and tidal sand banks and reveal the importance of sediment mixtures on the initial growth of these bedforms (Walgreen et al. 2004, Roos et al. 2007a).

More recently, Roos et al. (2007b) has investigated the grain sorting over offshore sand waves using a numerical model based on that of van den Berg & van Damme (2005). The model is fully nonlinear and is able to describe the growth of sand waves and the sorting process for large amplitudes of the bottom forms. In this respect, the model of Roos et al. (2007b) is a powerful tool to analyse the morphodynamic process under investigation. However, being based on a numerical approach which solves the nonlinear problem, the model is computationally expensive and the investigation of the parameter space implies high costs.

In the following we describe an analytical model able to investigate the initial stage of sand wave formation when a heterogenous sediment mixture is considered. In the next Section we formulate the problem. Subsequently, the interaction of a tidal cur-

rent with an arbitrary bottom perturbation is studied and the conditions leading to the appearance of sand waves are determined. Also the grain sorting process along the bottom forms is analysed. In Section 4, the results are described. Finally, in Section 5 some conclusions are drawn.

2 PROBLEM FORMULATION

2.1 Hydrodynamic problem

The hydrodynamic problem presently considered is similar to that described in Blondeaux & Vittori (2005 a,b) and Besio et al. (2006). For the sake of space their model will be only briefly summarized. The interested reader is referred to the previously mentioned papers for more details.

A shallow sea with a small depth h^*, in a horizontally unbounded domain is considered. A Cartesian coordinate system (x^*, y^*, z^*) is introduced in which the x^*- and y^*- axes are defined along the parallels pointing East and the meridian lines pointing North, respectively. The z^*- axes denotes the vertical axis and is directed upward such that $z^* = 0$ corresponds to the still water level. Hereinafter a star denotes a dimensional quantity. The water motions are described by means of continuity and momentum equations in which the contributions due to the Coriolis force are taken into account since they affect the tidal current. However, as discussed by Besio et al. (2006), when the interaction of the tidal current with a bottom waviness characterized by wavelengths of the order of hundreds of meters is analysed, the terms related to inertia and Coriolis effects can be neglected. The flow regime is assumed to be turbulent and viscous effects are neglected. Moreover, following the analysis of the review paper by Soulsby (1983), turbulence is assumed to be isotropic. Consequently, the Boussinesq hypothesis is adopted to model the Reynolds stresses and a scalar kinematic eddy viscosity ν_T^* is introduced.

The hydrodynamic problem can be made dimensionless using the undisturbed mean water depth h_0^* as length scale and the maximum value U_0^* of the depth averaged fluid velocity during the tidal cycle to scale the velocity components (u^*, v^*, w^*). Furthermore, the inverse of the angular frequency ω^* of the tide is used as time scale. Besides the values of Ω ($\Omega = \Omega^*/\omega^*$) and φ_0 (Ω^* denotes the angular velocity of the Earth rotation and φ_0 is the local latitude), the dimensionless hydrodynamic problem is characterized by two main dimensionless parameters,

$$r = \frac{U_0^*}{\omega^* h_0^*}, \qquad \delta = \frac{\sqrt{\nu_{T0}^* / \omega^*}}{h_0^*} \tag{1}$$

in which the constant ν_{T0}^* provides the order of magnitude of the eddy viscosity such that ν_T ($\nu_T = \nu_T^* / \nu_{T0}^*$) describes the temporal and spatial variations of the turbulence structure and is of order one. Presently, ν_T is chosen such that the eddy viscosity grows linearly with the distance from the bed and then decreases to achieve a finite small value at the free surface and it is assumed to be time independent. The Keulegan-Carpenter number r denotes the ratio between the amplitude of the horizontal fluid displacement oscillations and the local depth. The parameter δ represents the ratio between the thickness of the viscous boundary layer and the local water depth. Roughly estimated, δ turns out to be of order one. To close the hydrodynamic problem, kinematic and dynamic boundary conditions are forced at the free surface and the no-slip condition is required at a distance from the bed proportional to the dimensionless bottom roughness z_r ($z_r = z_r^*/h_0^*$).

2.2 Morphodynamic problem

The seabed is assumed to be made up of a cohesionless grain size mixture with N distinct grain size classes. Each class lays within the sand 'region' and is characterized by a grain size diameter d_i^* ($i = 1, .., N$). All grains have the same density ρ_s^* and the heterogeneous bed has a porosity n. The volume fraction of each grain size class is denoted by p_i. Since p_i is the volume percentage of each grain size class, it follows that

$$\sum_{i=1}^{N} p_i = 1 \tag{2}$$

The arithmetic mean grain size of the mixture is then defined as

$$d_m^* = \sum_{i=1}^{N} d_i^* p_i \tag{3}$$

Within the bed, each grain size class must satisfy the sediment continuity equation. For a sediment grain in the bed to be entrained into motion, it must be exposed to the action of the fluid motion. Therefore, the closer the grain is to the bed surface, the higher the probability is that it will be entrained. The simplest reasonable approximation of the probability of entrainment per unit time of a grain as a function of the elevation within the bed is a step function, according to which the probability of erosion of a grain per unit time has a constant value in an active layer of thickness L_a^* near the bed surface, and vanishes below this layer (Hirano 1971). The sediment within the top layer is assumed to be instantaneously well mixed and directly available for transport such that the volume fractions $p_{a,i}$ within the active layer can change in time but have no vertical structure. The layer underneath the active layer is called the sub-

strate. Within the substrate, the sediment is not directly available for transport and the volume fractions $p_{s,i}$ in the substrate are independent of time but can have an arbitrary vertical structure. In Figure 1 a sketch of the model geometry is provided.

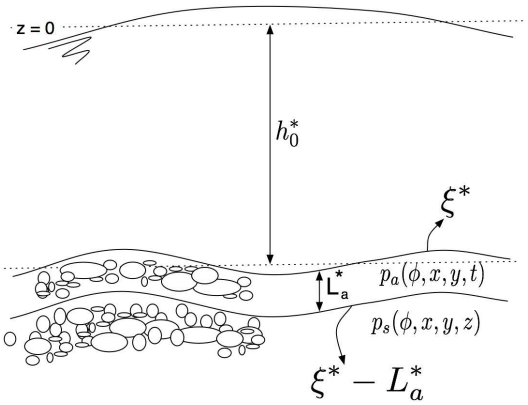

Figure 1. Sketch of the model geometry.

Deploying this approximation and making use of Leibniz' rule, the sediment continuity equation for each grain class is written as

$$(1-n)\left[p_{c,i} \frac{\partial(\xi^* - L_a^*)}{\partial t^*} + \frac{\partial(L_a^* p_{a,i})}{\partial t^*} \right] = - \frac{\partial(p_{a,i} Q_{x,i}^*)}{\partial x^*} - \frac{\partial(p_{a,i} Q_{y,i}^*)}{\partial y^*} \quad (4)$$

Here, $z^* = \xi^*$ denotes the seabed elevation, ($Q_{x,i}^*$, $Q_{y,i}^*$) represent the volumetric sediment transport rates per unit width and per unit fraction of the grain size class i, in the x- and y- directions respectively. Furthermore, $p_{c,i}$ is the volume fraction related to the grain size class i at the level $z^* = \xi^* - L_a^*$. The first term on the left hand side of Equation 4 models the interaction between the active layer and the substrate and

$$p_{c,i} = \begin{cases} p_{a,i} & if \quad \partial(\xi^* - L_a^*)/\partial t^* \geq 0 \\ p_{s,i} & \partial(\xi^* - L_a^*)/\partial t^* < 0 \end{cases} \quad (5)$$

The sediment continuity equation is then made dimensionless: ξ^* is scaled with the undisturbed water depth and the dimensionless sediment transport rates ($Q_{x,i}$, $Q_{y,i}$) are defined as

$$(Q_{x,i}, Q_{y,i}) = \frac{(Q_{x,i}^*, Q_{y,i}^*)}{\sqrt{(\rho_s^*/\rho^* - 1) g^* (d_i^*)^3}} \quad (6)$$

Moreover, since the bottom is assumed to be initially flat, L^*_a is scaled with the mean grain size in such a way that $L_a = L^*_a / d^*_{m0}$ is a quantity of order one. Hence Equation 4 becomes

$$p_{c,i} \frac{\partial \xi}{\partial t} - \Delta_{La} p_{c,i} \frac{\partial L_a}{\partial t} + \Delta_{La} \frac{\partial(L_a p_{a,i})}{\partial t} = - \Delta \left(\frac{d_i^*}{d_m^*} \right)^{3/2} \left[\frac{\partial(p_{a,i} Q_{x,i})}{\partial x} + \frac{\partial(p_{a,i} Q_{y,i})}{\partial y} \right] \quad (7)$$

where,

$$\Delta_{La} = \frac{d_{m0}^*}{h_0^*}, \qquad \Delta = \frac{d_{m0}}{(1-n)\sqrt{\psi_m}} \quad (8)$$

Here, $d_{m0} = d_{m0}^* / h_0^*$ represents the initial dimensionless mean grain size and ψ_m is the mobility number evaluated for the mean grain size

$$\psi_m = \frac{(\omega^* h_0^*)^2}{(\rho_s/\rho - 1) g^* d_{m0}^*} \quad (9)$$

Considering a mean grain size in the order of mm, a typical undisturbed water depth of 30 m and a semi-diurnal tide, it follows that Δ_{La} and Δ are of order 10^{-5} and 10^{-3}, respectively. The variables g^* and ρ^* are the gravitational acceleration and the sea water density, respectively.

To close the morphodynamic problem, the sediment transport rate should be specified. Presently, only the transport of sediments close to the bed (bedload) is considered and the weak effects due to the spatial variations of the bottom are taken into account: $(Q_{x,i}, Q_{y,i}) = (Q_{Bx,i}, Q_{By,i}) + (Q_{Px,i}, Q_{Py,i})$. Finally, the sediment transport in suspension is assumed to be negligible. The fractional bedload transport ($Q_{Bx,i}$, $Q_{By,i}$) is evaluated by means of the formula proposed by van Rijn (1993)

$$(Q_{Bx,i}, Q_{By,i}) = \frac{0.25}{R_{p,i}^{0.2}} \left(\frac{\theta_i - \theta_{b,i}^{cr}}{\theta_{b,i}^{cr}} \right)^{3/2} \frac{(\theta_{x,i}, \theta_{y,i})}{\sqrt{\theta_i}} \quad (10)$$

where $(\theta_{x,i}, \theta_{y,i})$ are the x- and y-components of the Shields parameter for the grain class i ($\theta_i = (\theta_{x,i}^2 + \theta_{y,i}^2)^{1/2}$), the critical shear stress $\theta^{cr}_{b,i}$ of the grain size class i is modified to take into account hiding/exposure effects and $R_{p,i} = ((\rho_s^*/\rho^* - 1) g^* d_i^{*3})^{1/2}/\nu$ is the particle Reynolds number of the grain class i. In particular, the critical shear stress related to the grain size class i is obtained by multiplying the critical shear stress of the mean diameter with the hiding function proposed by Ashida & Michiue (1972) such that $\theta^{cr}_{b,i} = H_i \, \theta^{cr}_{b,m}$ with

$$H_i = \begin{cases} \left[\dfrac{\log 19}{\log(19 d_i^*/d_m^*)} \right]^2 & if \quad d_i^*/d_m^* \geq 0.4 \\ 0.843 (d_m^*/d_i^*) & d_i^*/d_m^* < 0.4 \end{cases} \quad (11)$$

The critical shear stress related to the mean grain size is calculated by means of the expression given by Brownlie (1981). Note that the Shields parameter is evaluated at the top of the bedload layer as proposed by Colombini (2004).

The effect of small spatial variations of the bottom on the bedload transport is modeled by

$$\left(Q_{Px,i}, Q_{Py,i}\right) = Q_{B,i} G_i \left(\frac{\partial \xi}{\partial x}, \frac{\partial \xi}{\partial y}\right) \qquad (12)$$

where G_i is a dimensionless second order 2-D tensor, (e.g. Talmon et al. (1995), Seminara (1998)).

3 TIME DEVOLPMENT OF ARBITRARY BOTTOM PERTURBATIONS

To investigate the sediment sorting process corresponding with the initial formation of tidal sand waves, the stability of the flat bottom configuration to arbitrary bottom perturbations of small amplitude (strictly infinitesimal) is analysed by taking into account the effects of the grain size mixture. Consequently, we consider the seabed to differ from the flat one by a small amount proportional to ε and write the dimensionless water depth h as

$$h = 1 - \varepsilon \sum_n A_n(t) e^{i(\alpha_{nx} x + \alpha_{ny} y)} + O(\varepsilon^2) \qquad (13)$$

where α_{nx} and α_{ny} are the dimensionless wavenumbers in the x- and y- directions, respectively. The amplitude of the bottom perturbation is represented by $\varepsilon A(t)$ with $\varepsilon << 1$ and *c.c.* denotes the complex conjugate of a complex quantity. Since ε is much smaller than one, the solution can be expanded in terms of this small parameter. Subsequently, the problem is linearized in such a way that the different spatial components of the bottom perturbation evolve independently from each other. Then, the hydrodynamic problems at $O(\varepsilon^0)$ and $O(\varepsilon^1)$ consist of solving the flow induced by tide propagation over a flat and a wavy bottom, respectively, and do not differ from the problems addressed by Blondeaux & Vittori (2005a,b). The reader is referred to Blondeaux & Vittori (2005a,b) for a description of the solution procedure.

Once the flow field is known, the sediment transport rates per unit fraction at the leading and first order of approximation can be evaluated. Since the volume fractions are expanded with respect to ε too, it follows that

$$\left[Q_{Bx,i}, Q_{By,i}, Q_{Px,i}, Q_{Py,i}\right] = \left[Q_{Bx0,i}, Q_{By0,i}, Q_{Px0,i}, Q_{Py0,i}\right]$$

$$+\varepsilon A(t)\left[Q_{Bx1,i}, Q_{By1,i}, Q_{Px1,i}, Q_{Py1,i}\right] e^{i(\alpha_x x + \alpha_y y)}$$

$$+c.c. + O(\varepsilon^2), \qquad (14)$$

$$\left[p_{c,i}, p_{a,i}, p_{s,i}\right] = \left[p_{c0,i}, p_{a0,i}, p_{s0,i}\right] +$$

$$\varepsilon\left[p_{c1,i}, p_{a1,i}, p_{s1,i}\right] e^{i(\alpha_x x + \alpha_y y)} + c.c. + O(\varepsilon^2) \qquad (15)$$

Note that from Equation 15 it follows that

$$d_m^* = d_{m0}^* + \varepsilon A(t) d_{m1}^* e^{i(\alpha_x x + \alpha_y y)} + c.c. + O(\varepsilon^2) \qquad (16)$$

With Equations 7, 14 and 15, the sediment continuity equation for each grain size class can be written in the form

$$p_{a0,i} \frac{\partial A(t)}{\partial t} + \Delta_{La} L_{a0} \frac{\partial p_{a1,i} A(t)}{\partial t} = \Delta \gamma_i(t) A(t) \qquad (17)$$

in which an initially uniformly distributed bottom composition is considered, such that $p_{c0,i}$ is equal to $p_{a0,i}$. Moreover, L_{a0} is the dimensionless active layer thickness of the basic state which turns out to be of order 1.

Summation of Equation 17 over all grain size classes leads to an equation that describes the time development of the amplitude of the bottom perturbation

$$\frac{\partial A(t)}{\partial t} = \Delta \gamma(t) A(t), \qquad \gamma(t) = \sum_{i=N}^{N} \gamma_i(t) \qquad (18)$$

Resubstitution of Equation 18 into Equation 17 leads to

$$\frac{\Delta_{La} L_{ao}}{\Delta} \frac{\partial p_{a1,i}}{\partial t} = p_{a0,i} \gamma(t) - \gamma_i(t) \qquad (19)$$

Since Δ_{La}/Δ can be assumed to be much smaller than one, the time derivative of $p_{a1,i}$ in Equation 19 can be neglected. Then, using the constraint

$$\sum_{i=1}^{N} p_{a1,i} = 0 \qquad (20)$$

a linear system of N equations with N variables is obtained

$$a_i p_{a1,i} = b_i \qquad (21)$$

In Equation 21, a_i and b_i are found by making explicit the dependence of $\gamma(t)$ and $\gamma_i(t)$ on $p_{a1,i}$. Note that the critical value of the Shields parameter depends on the mean grain size (Eq. 12) such that also the expansion of $\theta^{cr}_{b,i}$ in terms of ε leads to a contribution to a_i.

The time development of the amplitude of the generic mode of the bottom perturbation is then given by

$$\frac{\partial A(T)}{\partial T} = \gamma(t) A(T) \qquad (22)$$

in which the slow morphodynamic time scale T ($T=t\Delta$) is introduced and $\gamma(t)$ is a periodic, complex function of t which depends on the parameters of the problem. The solution of Equation 22 shows that the growth or decay of the bottom perturbation is controlled by the real part $\langle\gamma\rangle_R$ of the time average $\langle\gamma\rangle$ (over a tidal cycle) of $\gamma(t)$. On the other hand, the imaginary part provides information concerning the migration of the bed forms. The remaining real and imaginary periodic parts (γ- $\langle\gamma\rangle$) of $\gamma(t)$ describe the oscillations of the bottom forms taking place during the tidal cycle around their average position.

4 RESULTS

In the following, we present the effects of a grain size mixture on the formation and main geometrical characteristics of tidal sand waves, along with the effects on the bed composition. Because our attention is focused on the effects of the non-uniformity of the sediment, values of the hydrodynamic parameters typical for the North Sea are considered and set as default values. The average water depth is assumed to be 30 m and the latitude has the fixed value of 51° North. Moreover, the M2 component is supposed to be the dominant tidal constituent with a maximum value of the depth-averaged fluid velocity equal to 0.7 m/s. Then, the Keulegan-Carpenter number r is equal to 161. The tidal velocity vector is counterclockwise rotating and the eccentricity, i.e. the ratio between the minor and major axis of the tidal ellipse, is 0.2. In all the forthcoming numerical experiments, these values are used for the hydrodynamic parameters unless explicitly stated otherwise. For an analysis of the influence of the hydrodynamic parameters on the phenomenon, the reader is referred to Besio et al. (2006).

To characterize the sediment mixture, the logarithmic phi-scale defined as $\varphi_i = - log_2(d_i^*/d_{ref}^*)$ is introduced. Here, d_i^* is the grain size diameter in units of mm and $d_{ref}^*=1$ mm. Observations show that most grain size mixtures are approximately normally distributed if plotted on the phi scale. Therefore, we can describe the sediment mixture by specifying φ_m and σ, i.e. the mean grain size and standard deviation related to the phi scale respectively. They are evaluated by

$$\varphi_m = \sum_i^N \varphi_i p_{\varphi,i}\,, \qquad \sigma^2 = \sum_{i=1}^N (\varphi_i - \varphi_m)^2 p_{\varphi,i} \qquad (23)$$

where $p_{\varphi,i}$ is the volume fraction of each grain size class related to the probability density function $p(\varphi)$. The corresponding geometric mean grain size is then given by $d_{gm}^*=2^{-\varphi m}$.

Since Besio et al. (2006) illustrated that the most amplified modes are those characterized by crests orthogonal to the main axis of the tidal ellipse, we focus our attention to this case. Therefore, we introduce the axes (x', y') such that x' is aligned with the main axis of the tidal ellipse and perturbations characterized by $\alpha_{y'}$ equal to zero are considered. Moreover, due to the symmetry of the forcing flow, no migration of the bottom forms is expected and indeed $\langle\gamma\rangle_I$ vanishes.

First, we investigate the effect of describing the mixture more or less accurately, i.e. using different values of N. Figure 2 shows the amplification rate $\langle\gamma\rangle_R$ as a function of $\alpha_{x'}$ for a uniform sediment and for sediment mixtures described by two, three, six and ten grain size classes. In all cases, the geometric mean grain size is equal to 0.6 mm and the standard deviation of the sediment mixtures is fixed equal to 0.1. Note that a relatively coarse geometric mean grain size is considered, as sand ripples are more likely to be absent in this case. Moreover, the value of U_0^* is chosen such that the sediment transport in suspension, presently discarded, is effectively negligible. Figure 2 shows that the flat bed configuration is more unstable for a uniform bed than for a heterogeneous sediment mixture and the wavelength of the most amplified mode appears to be shorter.

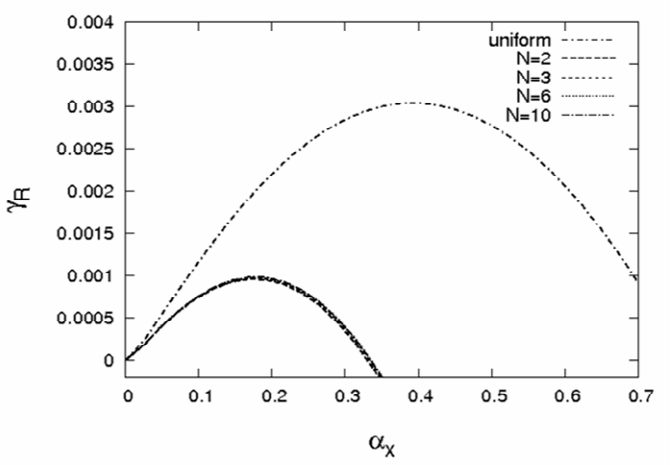

Figure 2. The growth rate $\langle\gamma\rangle_R$ plotted as a function of $\alpha_{x'}$ for a uniform sediment and for sediment mixtures described by two, three, six and ten grain size classes. In all cases d_{gm}^* is equal to 0.6 mm and the standard deviation of the heterogeneous sediment mixtures is fixed equal to 0.1.

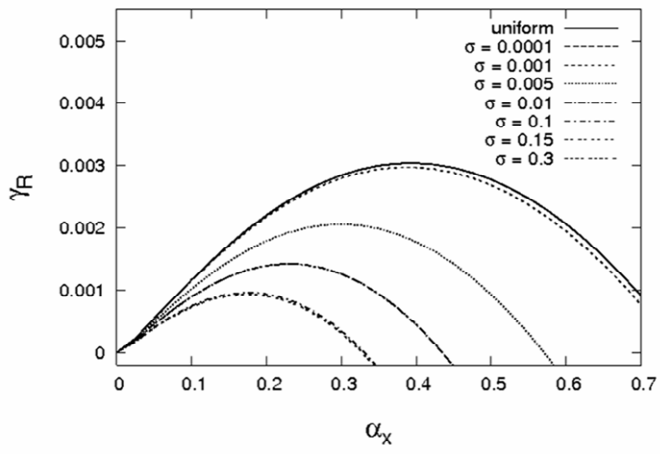

Figure 3. The growth rate $\langle \gamma \rangle_R$ plotted as a function of α_x for a uniform sediment and for bimodal sediment mixtures with different amount of sortedness. The value of σ is changed between 0.0001 and 0.3. In all cases d_{gm}^* is equal to 0.6 mm.

Moreover, it is found that an increase of N, i.e. a more detailed description of the bed composition, leads only to small quantitative differences. Therefore to keep the analysis of the results as clear as possible, in the following experiments concerning the formation of sand waves, only bimodal mixtures will be considered.

To investigate the influence of the standard deviation σ, the growth rate $\langle \gamma \rangle_R$ is plotted versus α_x, for sediment mixtures that are more or less well sorted but characterized by the same geometric mean grain size d_{gm}^*=0.6 mm (Figure 3). A clear stabilizing effect on the growth rate is found when the standard deviation increases. In particular the largest effect is found when σ passes from 0.001 to 0.15. Of course, when σ tends to vanish, the results of the uniform case are recovered. Additionally, the results of Figure 3 reveal that the sand waves which appear for a graded sediment tend to be longer than those found

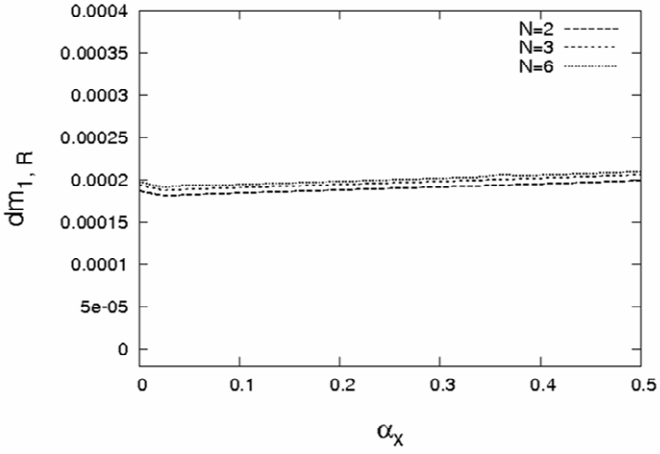

Figure 4. The value of $\langle d_{m1} \rangle_R$ plotted as a function of α_x for sediment mixtures described by two, three and six grain size classes. In all cases d_{gm}^* is equal to 0.6 mm and the value of σ is fixed equal to 0.1.

considering a uniform sediment. Similar results are found for sediment mixtures characterized by different geometric mean grain size and for bimodal mixtures with the same geometric mean grain size but changing the Keulegan-Carpenter number (not shown). At this point, the spatial variation of the bed composition related to the bed elevation is considered. From Equation 15 it follows that the real part $d_{m1,R}^*$ of d_{m1}^* describes variations of the mean grain size which are in or out of phase with the elevation of the bottom while the imaginary part is related to a shift of the grain size distribution with respect to the bottom forms. Since the problem is symmetric, the imaginary part $\langle d_{m1}^* \rangle_I$ of the time average $\langle d_{m1}^* \rangle$ of d_{m1}^* vanishes. In Figure 4 the value of the time average of the real part of $d_{m1} = d_{m1}^*/d_{m0}^*$ is plotted as a function of α_x, for sediment mixtures characterized by d_{gm}^*=0.6 mm and a standard deviation equal to 0.1. The accuracy of the description of the sediment mixtures is varied and mixtures modeled by two, three and six different grains size classes are considered. Again, it appears that describing the bed composition more accurately provides no qualitative different result. Moreover, $\langle d_{m1} \rangle_R$ is found positive for all experiments, indicating a coarsening of the sediment at the crest and a fining at the trough of the bottom forms. Finally, the value of $\langle d_{m1} \rangle_R$ corresponding to the fastest growing wavenumber for bimodal sediment mixtures and different amounts of sortedness is shown in Figure 5. It is found that the amount of sortedness of a sediment mixture does not qualitatively influence the value of $\langle d_{m1} \rangle_R$ and a coarsening at the crest and a fining at the trough is observed.

To ascertain that the results previously described are not due to the use of a particular empirical sediment transport predictor, the analysis described above is also performed using the sediment transport formula proposed by Meyer-Peter & Muller (1948) such that the fractional bedload transport is evaluated by

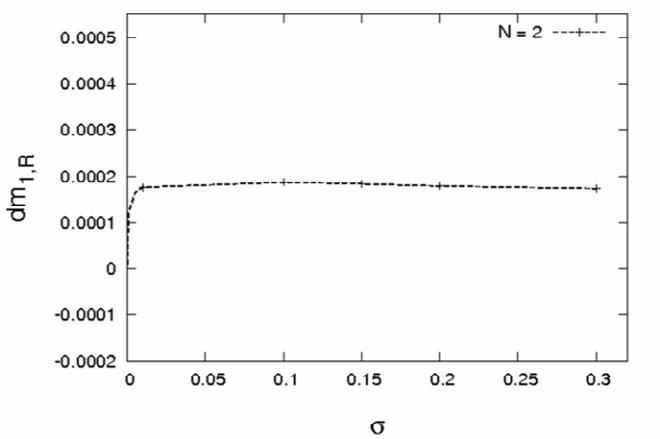

Figure 5. The value of $\langle d_{m1} \rangle_R$ corresponding to the fastest growing wavenumber for bimodal sediment mixtures and different amounts of sortedness. In all cases d_{gm}^* is equal to 0.6 mm.

$$(Q_{Bx,i}, Q_{By,i}) = 8(\theta_i - \theta_{b,i}^{cr})^{1.5} \frac{(\theta_{x,i}, \theta_{y,i})}{\theta_i} \quad (24)$$

In Figures 6 and 7, the results using Meyer-Peter & Muller's formula are illustrated. Figure 6 presents the growth rate plotted versus α_x, for a uniform sediment and for bimodal sediment mixtures characterized by a geometric mean grain size equal to 0.6 mm, considering different values of the standard deviation. The results show a clear stabilizing effect when the value of σ is increased. Moreover, the wavelength is found to increase for heterogeneous sediment mixtures.

Figure 7 presents the value of $\langle d_{m1} \rangle_R$ as a function of α_x, for the same bimodal mixtures considered in Figure 6. Also using Meyer-Peter & Muller's formula, the real part of the time average of d_{m1} turns out to be positive, regardless of the value of σ.

Hence, the qualitative findings of the proposed model seem robust with respect to the use of different sediment transport predictors.

Unfortunately, a detailed quantitative comparison of the theoretical results with field measurements concerning the sediment sorting cannot be made. This is partial due to the limitations of the model and to the paucity of field observations. Indeed, the model presented in this paper considers the seabed to be without ripples such that only grain size mixtures with a relative coarse mean grain size can be considered. Moreover, only relatively moderate values of the Keulegan-Carpenter number can be considered, since the transport of sediment in suspension is presently neglected. Although these limitations, the model does seem to capture the grain size sorting process. Indeed the theoretical predicted coarsening at the crest is in partial qualitative agreement with the observations described by Roos et al. (2006b). In this respect the authors feel that a description of the phenomenon also for larger Keulegan-Carpenter numbers could model the sediment fining at the crests of sand waves observed at some locations.

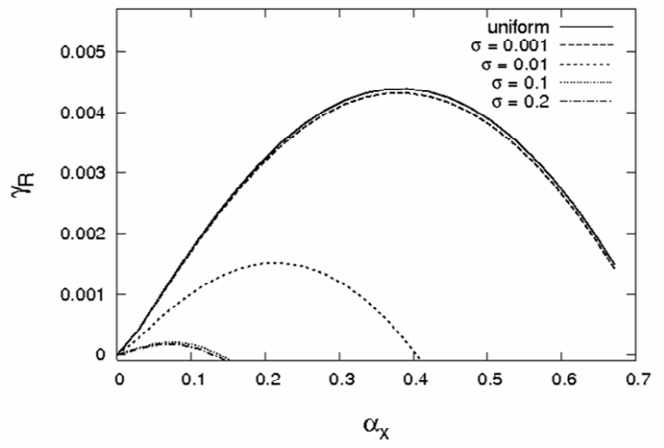

Figure 6. The growth rate plotted as a function of α_x, for a uniform sediment and for bimodal sediment mixtures with different amount of sortedness. The value of σ is changed between 0.001 and 0.2. In all cases d_{gm}^* is equal to 0.6 mm. The result are obtained using the bedload transport predictor proposed by Meyer-Peter & Muller (1948).

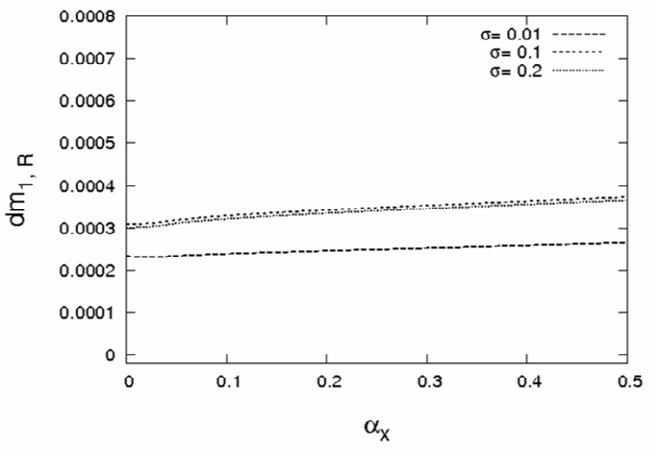

Figure 7. The value of $\langle d_{m1} \rangle_R$ plotted as a function of α_x, for bimodal sediment mixtures with different amount of sortedness (σ = 0.01, σ = 0.1, σ = 0.2). In all cases d_{gm}^* is equal to 0.6 mm. The result are obtained using the bedload transport predictor proposed by Meyer-Peter & Muller (1948).

Furthermore, the presently described results are in qualitative agreement with the results of Foti & Blondeaux (1995b) who, using both a theoretical analysis and experimental observations, showed that the sea ripple growth is inhibited by a graded sediment and the ripples which appear tend to be longer than those observed for a uniform bottom composition.

5 CONCLUSIONS

In this paper, a model is developed to study the initial formation of sand waves in shallow tidal seas characterized by a bottom made up of a sediment mixture.

The main goal of the work was the investigation of the sorting process induced by the incipient growth of sand waves and the evaluation of the effects that a graded sediment has on the formation of the bottom forms.

The analysis shows that for moderate values of *r*, i.e. for moderate tidal strengths, the graded sediment tends to stabilize the flat bottom configuration. Moreover, it is found that the coarse fraction moves towards the crests and the fine fraction to the troughs. Finally, the results show that a more or less accurate description of the sediment mixture, i.e. a description of the mixture with more or less grain size classes, has no qualitative influence on the results.

Use is made of two different sediment transport predictors and no qualitatively different result is obtained. Hence, the model does not seem to depend on the use of a particular sediment transport formula.

Furthermore, the present theoretical results are partially in agreement with the field observations described in Roos et al. (2007b).

The ongoing research aims at removing some of the limitations previously described. First, we want to take into account the time derivative of $p_{a1,i}$ in Equation 19 in such a way that grain size mixtures within the whole sand region can be considered. Secondly, the fractional transport of sediment in suspension needs to be modeled such that the phenomenon can also be described for large Keulegan-Carpenter numbers. Finally, a more detailed comparison of the model results with field data is necessary to support the model findings.

ACKNOWLEDGEMENTS

This research has been supported by the Ministero dell'Universita e della Ricerca under the contracts n. 2005080197 (Cave sottomarine e ripascimenti: modellazione morfologica e applicazioni). Initial stage funding was also provided by the University of Genoa. The youngest author (T. v O.) wishes to acknowledge the E.U. for a grant in the framework of the FLUBIO project.

REFERENCES

Antia, E.E. 1996. Shoreface-connected ridges in German and US mid-Atlantic bights: similarities and contrasts. *J. Coast. Res.* 12: 141-146

Ashida, K. & Michiue, M. 1972. Study on hydraulic resistance and bedload transport rate in alluvial streams. *Japan Society of Civil Engineering* 206: 59-69.

van den Berg, J. & van Damme, R.M.J. 2005. Sand wave simulation on large domains. In Gary Parker and Marcelo Garcia (ed.), *4th IAHR Symposium on River, Coastal and Estuarine Morphodynamics, Illinois, 2005*.

Besio, G., Blondeaux, P. & Vittori, G. 2006. On the formation of sand waves and sand banks. *J. Fluid Mech.* 557: 1-27.

Blondeaux, P. & Vittori, G. 2005a. Flow and sediment transport induced by tide propagation: 1. The flat bottom case. *J. Geophys. Res.* 110(C7).

Blondeaux, P. & Vittori, G. 2005b. Flow and sediment transport induced by tide propagation: 1. The wavy bottom case. *J. Geophys. Res.* 110(C7).

Brownlie, W.R. 1981. Prediction of flow depth and sediment discharge in open channels. *Rep. n. KH-R-43A*. W. M. Keck Lab. of Hydraulics and Water Resources, California Institute of Technology, Pasadena, California

Colombini, M. 2004. Revisiting the linear theory of sand dune formation. *J. Fluid Mech.* 502: 1-16.

Foti, E. & Blondeaux. P. 1995a. Sea ripple formation: the turbulent boundary layer case. *Coastal Engineering.* 25 (3-4): 227-236

Foti, E. & Blondeaux, P. 1995b. Sea ripple formation: the heterogeneous sediment case. *Coastal Engineering.* 25 (3-4): 237-253

Gao, S., Collins, M.B., Lanckneus, J, De Moor, G. & Van Lancker, V. 1994, Grain-size trends associated with net sediment transport patterns: an example from the Belgian continental shelf. *Mar. Geol.* 121: 171-185

Hirano, M. 1971. River bed degradation with armouring. *Trans. Jpn. Soc. Civ. Eng.* 3: 194-195

Houthuys, R., Trentesaux, A. & De Wolf, P. 1994. Storm influences on a tidal sandbank's surface (Middelkerke bank, southern North Sea). *Mar. Geol.* 121: 1-21

Lanckneus, J., De Moor, G. & Stolk, A. 1994. Environmental setting, morphology and volumetric evolution of the Middelkerke bank (southern North Sea). *Mar. Geol.* 121: 1-21

Meyer-Peter, E. & Muller, R. 1948. Formulas for bedload transport. *Proc. 2nd congress I.A.H.R., Stockholm, 1948.* 39-64

van Rijn, L.C. 1993. Principles of sediment transport in rivers, estuaries and coastal seas, Amsterdam: Aqua Publ.

Roos, P.C., Wemmenove, R., Hulscher, S.J.M.H. & Hoeijmakkers, H.W. M. & Kruyt, N.O. 2007a. Modeling the effect of non-uniform sediment on the dynamics of offshore tidal sand banks, *J. Geophys. Res.* 112

Roos, P.C. & Hulscher, S.J.M.H. & van der Meer, F. & van Dijk, T.A.G.P. & Wientjes, I.G.M. & van den Berg, J. 2007b. Grain size sorting over offshore sandwaves: Observations and modeling. In Marjolein Dohmen-Janssen and Suzanne Hulscher (ed.), *5th IAHR Symposium on River, Coastal and Estuarine Morphodynamics, Twente, 2007*.

Seminara, G. 1998. Stability and morphodynamics. *Meccanica*. 33: 59-99

Soulsby, R.L. 1983. The bottom boundary layer of shelf seas. In B. John (ed.) *Physical Oceanography of Coastal and Shelf seas* Elsevier: 189-266

Swift, D.J.P., Parker, G., Lanfredi, N.W., Perillo, G. & Figge, K. 1978. Shoreface-connected sand ridges on American and European shelves: a comparison. *Estur. Coast. Mar. sci.* 7: 257-273

Talmon, A.M. & Struiksma, N. & van Mierlo, M.C.L.M. 1995. Laboratory measurements of the direction of sediment transport on transverse alluvial-bed slopes. *J. Hydraul. Res.* 33: 495-517

Van Lancker, V. 1999. Sediment and morphodynamics of a siliciclastic near coastal area, in relation to hydrodynamical and meteorological conditions: Belgian continental shelf. *PhD thesis*, Univ. Gent, Belgium

Vincent, C.E., Stolk, A. & Porter, C.F.C. 1998. Sand suspension and transport on the Middelkerke bank (southern North Sea) by storms and tidal currents. *Mar. Geol.* 150: 113-129

Walgreen, M., de Swart, H.E. & Calvete, D. 2004. A model for grain-size sorting over tidal sand ridges. *Ocean Dynamics* 54 (3-4)